

## **DIFFERENTIAL SCANNING CALORIMETRY STUDIES ON INFLUENCE OF MICROSTRUCTURE ON TRANSFORMATION OF $\gamma\text{-Fe}_2\text{O}_3$ TO $\alpha\text{-Fe}_2\text{O}_3$**

*A. C. Vajpei, F. Mathieu, A. Rousset\*, F. Chassagneux\*\*,  
J. M. Letoffe\*\*\* and P. Claudy\*\*\**

LABORATOIRE DE CHIMIE DES MATERIAUX INORGANIQUES,  
UNIVERSITE PAUL SABATIER, 118 ROUTE DE NARBONNE,  
F-31062 TOULOUSE CEDEX, FRANCE

\*\*LABORATOIRE DE CHIMIE MINERALE III, UNIVERSITE CLAUDE BERNARD,  
43 BOULEVARD DU 11 NOVEMBRE 1918, F-69622 VILLEURBANNE  
CEDEX, FRANCE

\*\*\*LABORATOIRE DE THERMOCHIMIE MINERALE I.N.S.A.-U.A. 116,  
20 AVENUE ALBERT EINSTEIN, F-69621 VILLEURBANNE  
CEDEX, FRANCE

(Received June 10, 1986)

The transition  $\gamma\text{-Fe}_2\text{O}_3 \rightarrow \alpha\text{-Fe}_2\text{O}_3$  has been investigated in oxygen and argon using DSC measurements in the temperature range 298 to 820 K. The results have been interpreted by taking into account the method of preparation, the specific microstructure of the samples and the nature of the gas used. It has been shown that the transformation temperature, and in general the absolute value of the negative enthalpy of the transformation as well, rises with increase of the specific surface area of the  $\gamma\text{-Fe}_2\text{O}_3$ . The observed fluctuations in this trend are attributed to differences in the microporosity, gas sensitivity and crystallinity of the samples.

The reactivity of  $\gamma\text{-Fe}_2\text{O}_3$  towards its transformation to  $\alpha\text{-Fe}_2\text{O}_3$  is greatly affected by the method of preparation and pretreatment of the samples. Several studies have been made to elucidate these effects, which may profoundly influence the nature of the transformation  $\gamma\text{-Fe}_2\text{O}_3 \rightarrow \alpha\text{-Fe}_2\text{O}_3$  [1-10]. Thus, from their DTA studies in vacuum on  $\gamma\text{-Fe}_2\text{O}_3$  preparations, Bandó et al. [2] determined that the  $\gamma \rightarrow \alpha$  transformation took place in the range 400-500° for acicular aggregated particles, and at 450-500° for equiaxial separated unitary particles. Imaoka [3] observed that the  $\gamma \rightarrow \alpha$  transformation occurs in the range 250-400° for non-acicular particles, and at 560-650° for acicular particles. The thermodynamic and kinetic data, such as the heat of the transformation and the energy of activation, reported by several workers for the transformation  $\gamma\text{-Fe}_2\text{O}_3 \rightarrow \alpha\text{-Fe}_2\text{O}_3$ , also

\* Paper presented at the World Conference on Thermal Analysis, Madeira (Portugal), 1986.

\* Author to whom all correspondence should be addressed.

showed a large spread [1, 4–8]. The failure to obtain consistent results has been attributed, among other factors, to the presence of impurities [5], to the influence of the particle size [1, 5–8], and also to the various extents of ordering of the vacancies in the defect structure of  $\gamma$ -Fe<sub>2</sub>O<sub>3</sub> [7–8].

The effect of high pressure on the  $\gamma \rightarrow \alpha$  transformation of Fe<sub>2</sub>O<sub>3</sub> was studied by Goto [9] and it was shown that the rate constant depends principally on the thermodynamic parameter  $P\Delta V$ , where  $\Delta V$  is the volume difference between the  $\gamma$  and  $\alpha$  forms. Mechanochemical effects of pressing, vibromilling and low-temperature annealing of  $\gamma$ -Fe<sub>2</sub>O<sub>3</sub> on its transformation to  $\alpha$ -Fe<sub>2</sub>O<sub>3</sub> were investigated by Senna and coworkers [10a, b & c]. Using DSC measurements, they showed that the liberation of the stored energy of vibromilled  $\gamma$ -Fe<sub>2</sub>O<sub>3</sub> occurs through the recovery or recrystallization of the original  $\gamma$ -phase and its transition to  $\alpha$ -Fe<sub>2</sub>O<sub>3</sub> [10b]. At temperatures lower than 400°, recovery/recrystallization occurs favourably, whereas at above 400° predominantly the  $\gamma \rightarrow \alpha$  transition takes place [10b]. In another study involving DSC measurements, Senna [10c] examined the distinct effects of pressing and vibromilling on the rate and mechanism of the  $\gamma \rightarrow \alpha$  transformation for commercial  $\gamma$ -Fe<sub>2</sub>O<sub>3</sub> specimens. It was found that both these effects enhance the reactivity of  $\gamma$ -Fe<sub>2</sub>O<sub>3</sub>, but modify the microstructure of  $\gamma$ -Fe<sub>2</sub>O<sub>3</sub> in different ways.

As a continuation of our previous studies [1], the present paper reports the results of DSC measurements on the  $\gamma \rightarrow \alpha$  transformation, and compares and correlates the thermal features with the microstructural variations in submicronic  $\gamma$ -Fe<sub>2</sub>O<sub>3</sub> prepared by two different routes.

## Experimental

DSC measurements were carried out in oxygen and argon atmospheres, in the temperature range 298 to 920 K, at a heating rate of 5 deg min<sup>-1</sup>, by using a Mettler TA 2000 B heat flow DSC apparatus. Calibrations were made using the melting points and enthalpies of melting of high-purity metals [11].

Submicronic  $\gamma$ -Fe<sub>2</sub>O<sub>3</sub> samples were obtained by two different routes. First, hydrous magnetites were prepared by the neutralization of mixed solutions of one part of iron(II) chloride and two parts of iron(III) chloride with aqueous ammonia solution under an atmosphere of N<sub>2</sub> gas. These were dried and heated in a H<sub>2</sub>—H<sub>2</sub>O atmosphere at temperatures in the range 200 to 300°, followed by heating in air at 250° for 1 hour. Samples A, B and C series II were obtained by the decomposition of iron(II) oxalate dihydrate in air at 300, 400 or 800°, respectively, followed by their reduction in a H<sub>2</sub>—H<sub>2</sub>O atmosphere at 290, 310 or 360° for 2 hours, and oxidation in air at 300° for 1 hour.

The average diameter of the particles was obtained by using data from line-broadening measurements in powder XRD. For some selected samples, transmission electron microscopic and surface area measurements using the BET method were also carried out.

The stoichiometry and purity of the samples were checked by chemical analysis. In some cases of interest, TG and DTA measurements were also performed. The search for  $\text{Fe}^{2+}$  proved to be negative in the samples at the limits of detection of the methods used.

## Results and discussion

Table 1 summarizes the results of DSC measurements on the samples of series I and series II. Figures 1 and 2 depict some representative DSC curves obtained for the samples of series I and series II, respectively.

By inspection of Table 1 and the DSC curves in Figs 1 and 2, the following features are observed:

1. Corresponding to the transformation  $\gamma\text{-Fe}_2\text{O}_3 \rightarrow \alpha\text{-Fe}_2\text{O}_3$ , the samples of series I display a sharp and well-defined exothermic peak, while for the samples of series II a broad and rather diffuse effect is obtained. A weak and subtle divergence from the baseline, before the transformation, persists for the samples of series I. However, the effect is much more pronounced, particularly in oxygen, for the samples of series II.

**Table 1** Results of DSC measurements on  $\gamma\text{-Fe}_2\text{O}_3$  samples of series I and series II, in argon and oxygen atmospheres

S.N.	Samples $\langle D \rangle^*$ , Å	Atmosphere used: argon (Ar) or oxygen ( $\text{O}_2$ )							
		Onset temperature, °C, $\pm 1$ °C		Peak temperature, °C, $\pm 1$ °C		Peak-width at half-height, °C, $\pm 1$ °C		$-\Delta H$ , J/g, $\pm 3$ J/g	
		Ar	$\text{O}_2$	Ar	$\text{O}_2$	Ar	$\text{O}_2$	Ar	$\text{O}_2$
Series I									
1	300	493	498	500	508	7.7	8.5	149	139
2	320–340	490	494	500	503	7.1	7.7	143	139
3	400–450	484	490	490	498	7.7	7.8	141	139
4	550–600	487	499	495	508	9.4	8.9	129	139
Series II									
A	650	402	412	440	445	33	33	126	106
B	750–800	380	403	440	450	56	48	196	112
C	1000–1200	345	364	405	420	67	58	180	96

\* Average diameter of particles determined from line-broadening in powder X-ray diffraction, using the Scherrer method.

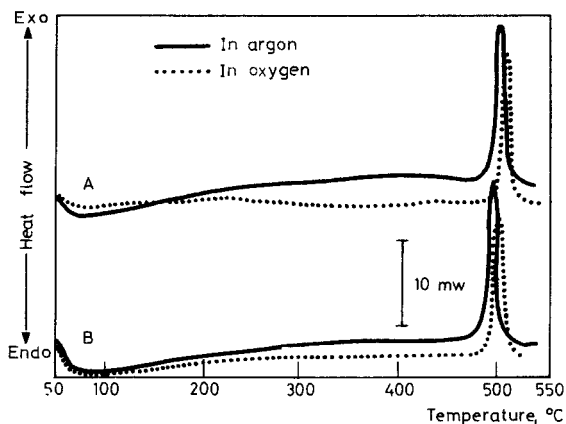


Fig. 1 DSC curves for (A) sample 1 and (B) sample 3, of series I in argon and oxygen atmosphere

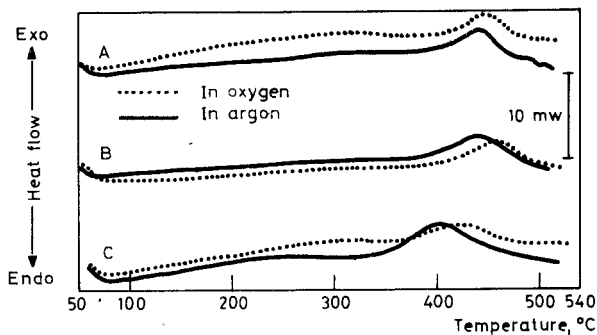


Fig. 2 DSC curves for (A) sample A, (B) sample B, and (C) sample C of series II, in argon and oxygen atmosphere

2. The peak-widths at the half-height for the samples of series I are quite comparable within the series, and are not observably affected by argon and oxygen atmospheres. However, they show a variation for the samples within series II. They are much the same in oxygen and in argon for sample A, but are different for samples B and C.

3. For both the initial and the final temperatures of the transformation  $\gamma\text{-Fe}_2\text{O}_3$  to  $\alpha\text{-Fe}_2\text{O}_3$ , considerable variations occur for the samples in series II, but much smaller ones for the samples of series I. Invariably, the temperatures are lower for the series II samples than those for the series I samples.

4. The transformation temperatures observed in oxygen atmosphere are always slightly higher than those observed in argon atmosphere.

5.  $-\Delta H$ , the energy released during the transformation, is larger when the reaction occurs in argon than for that in oxygen. Differences between the  $-\Delta H$

values in the two atmospheres for the samples of series I are small as compared to those observed for the samples of series II.

6. The heats of the transformation for the samples of series I in oxygen are virtually constant. The heats of transformation for the same samples in argon show subtle variations within the series. The heats of transformation for the samples of series II in oxygen are slightly different, but in argon considerable variations in the  $-\Delta H$  values are observed.

A brief consideration of the microstructural features of the samples, as revealed by electron microscopy and BET surface area measurements, is in place before as attempt to understand their overall thermal behaviour.

In fact, the samples of series I, derived from hydrous magnetites, display a narrow size distribution and are characterized by an equiaxial morphology of discrete individual particles possessing well-separated edges. The samples of series II possess a relatively broad size distribution and show a range of aggregated particles with acicular morphology, a continuous coherent sheet-like character and a flaky microporous texture.

Typically, sample 3 of series I had an average size of 510 Å and a specific surface area of 20 m<sup>2</sup>/g. After undergoing the  $\gamma \rightarrow \alpha$  transition in argon and oxygen atmospheres, it had a specific surface area of 15.2 m<sup>2</sup>/g and 13.5 m<sup>2</sup>/g, respectively. Electron microscopic examinations revealed that the  $\gamma$ -Fe<sub>2</sub>O<sub>3</sub> particles corresponding to these surface areas have average sizes of 530 Å and 840 Å, respectively.

For the samples of series I, the observation of a sharp and intense exothermic peak is associated with the initial surface nucleation of  $\alpha$ -Fe<sub>2</sub>O<sub>3</sub> and its growth from discrete homogeneous units of  $\gamma$ -Fe<sub>2</sub>O<sub>3</sub>. Due to their crystalline character, a sharp  $\gamma \rightarrow \alpha$  transition is thus displayed at higher temperatures.

For the samples of series II, the appearance of the broad and diffuse effect points to a different nature of the transformation. This presumably arises through the averaging and overlapping of various sluggish thermal effects emerging from a range of environments of nucleating species within the microporous texture. The coherence and high microporosity of the samples certainly permit the diffusion-inducing synchroshear of iron ions at temperatures much lower than for the samples of series I. Moreover, the higher microporosity causes a large amount of surface energy storage in these samples. This is liberated in the recrystallization of  $\gamma$ -Fe<sub>2</sub>O<sub>3</sub> itself, as shown by the baseline divergences before the  $\gamma \rightarrow \alpha$  transition, and in the form of excess energy stimulating the  $\gamma \rightarrow \alpha$  transition.

For the samples of series I in argon, a steady increase in  $-\Delta H$  with increasing surface area is observed. In oxygen atmosphere, however, the  $-\Delta H$  values are not much different. It is postulated that oxygen modifies the interface processes by causing increased ordering and recrystallization of  $\gamma$ -Fe<sub>2</sub>O<sub>3</sub> before the  $\gamma \rightarrow \alpha$  transition. Hence, almost similar thermal behaviour results for the transition in

oxygen atmosphere. In argon, failure to remove trace water present may have a catalysing effect on the  $\gamma \rightarrow \alpha$  transition, and dissipation of heat in the rapid exothermic reaction prevents the surface area from being reduced as much as observed in the case of oxygen during the  $\gamma \rightarrow \alpha$  transition. Also, the suppression of grain-growth before and after the transition in argon causes the transition to occur at lower temperatures and with the release of larger  $-\Delta H$ . For the samples of series II, due to the different extents of microporosity prevailing in the samples, despite the possible recrystallization in oxygen, the thermal behaviour is quite reflective of the subtle differences between the samples. Here, it is to be stressed that both the temperature and the  $-\Delta H$  values are affected not only by the particle profiles, but also by the microporosity, ordering, loosening and strengthening of the lattice in oxygen and argon atmospheres. For example, for the samples of series II, with decreased size, a recrystallization of  $\gamma\text{-Fe}_2\text{O}_3$  probably occurs, thereby causing an increase in the temperature of the transformation and a decrease in the  $-\Delta H$  values.  $-\Delta H$ , the energy released during the transformation, is always more in argon as it is not diverged much in recrystallization. In oxygen, with the growth of the  $\alpha\text{-Fe}_2\text{O}_3$  particles with reduced surface area as compared to that produced in argon, the transition temperatures are always higher and the  $-\Delta H$  values always lower than those observed in argon, due to the strained nature of  $\gamma\text{-Fe}_2\text{O}_3$  in argon. The differences in width of the DSC curves at half-height may also be explained in terms of the occupancy of the nucleation sites. For the samples of series I, therefore, the saturation of the nucleation sites corresponds to a sharp peak, while different degrees of inhomogeneities and alternating occupancies of nucleation sites in the microporous texture of series II samples may result in a wide variety of broadened and diffuse thermal effects, as is indeed observed in both argon and oxygen atmospheres.

In conclusion, the  $\gamma \rightarrow \alpha$  transition for  $\gamma\text{-Fe}_2\text{O}_3$  particles obtained by two different routes is greatly dependent on the nature of the samples, their morphology, microporosity and particle profiles. The inequivalence observed in the overall thermal behaviour of the samples in both argon and oxygen atmospheres is only tentatively correlated with the microstructure of the samples. Further studies are warranted and are being pursued with a view to quantifying the role of water and the effects of microporosity and gas sensitivity during the  $\gamma \rightarrow \alpha$  transformation.

\* \* \*

The authors are grateful to Mr. Christian Sarda for his help during the sample preparation and characterization, and to Mr. B. Maachi and Dr. M. Gougeon for their help in surface area measurements. A. C. Vajpei expresses his gratefulness for the award of a Postdoctoral Fellowship in Materials Science by the French Government, made through the Indo-French Scientists' Exchange Programme.

## References

- 1 A. Rousset, G. Boissier, J. P. Caffin and F. Chassigneux, C.R. Acad. Sc. Paris, 299 Ser. II (1984) 781.
- 2 Y. Bando, M. Kiyama, T. Takada and S. Kachi, Japan J. Appl. Phys., 4 (1965) 240.
- 3 Y. Imaoka, J. Electrochem. Soc. Japan, 36 (1968) 15.
- 4 W. Feitknecht and U. Mannweiler, Helv. Chim. Acta, 50 (1967) 570.
- 5 A. Ferrier, C.R. Acad. Sci., Paris, 264 c (1967) 819.
- 6 J. M. Trautmann, Bull. Soc. Chim. Fr., 3 (1966) 992.
- 7 A. H. Morrish, G. A. Sawatzky, in Proc. Int. Conf. Ferrites (Editors: Y. Hoshino, S. Iiida, and M. Sujimoto) University Park, Tokyo, 1967, p. 144.
- 8 A. V. Korobeinikova, V. I. Fadeeva and L. A. Reznitskii, J. Structural Chem., 17 (1976) 737.
- 9 Y. Goto, Japan. J. Appl. Phys., 3 (1964) 739.
- 10 (1) M. Senna and H. Kuno, J. Am. Ceram. Soc., 56 (1973) 492; (b) H. Imai and M. Senna, J. Appl. Phys., 49 (1978) 4433; (c) M. Senna, J. Appl. Phys., 49 (1978) 4580.
- 11 P. Claudy, B. Bonnetot, G. Chahine and J. M. Letoffe, Thermochim. Acta, 38 (1980) 75.

**Zusammenfassung** — Der Übergang  $\gamma\text{-Fe}_2\text{O}_3 \rightarrow \alpha\text{-Fe}_2\text{O}_3$  in Sauerstoff- und Argonatmosphäre wurde mittels DSC im Temperaturbereich von 298–820 K untersucht. Die Ergebnisse werden unter Berücksichtigung der Präparationsmethode, der spezifischen Mikrostruktur der Proben und der Natur des benutzten Gases interpretiert. Die Phasenumwandlungstemperatur und im allgemeinen die Absolutwerte der negativen Enthalpie der Phasenumwandlung erhöhen bzw. vergrößern sich mit steigender spezifischer Oberfläche des  $\gamma\text{-Fe}_2\text{O}_3$ . Die in diesem Trend auftretenden Fluktuationen werden Unterschieden in der Mikroporosität, der Gasempfindlichkeit und der Kristallinität der Proben zugeschrieben.

**Резюме** — Методом дифференциальной сканирующей калориметрии в атмосфере кислорода и аргона изучен фазовый переход  $\gamma\text{-Fe}_2\text{O}_3 \rightarrow \alpha\text{-Fe}_2\text{O}_3$  в интервале температур 298–820 К. Интерпретация результатов проведена с учетом метода получения, специфической микроструктуры образцов и типа используемой газовой атмосферы. Показано, что как температура превращения, так и абсолютное значение отрицательной энтальпии превращения увеличиваются с увеличением удельной площади поверхности образца  $\gamma\text{-Fe}_2\text{O}_3$ . Наблюдаемые при этом некоторые отклонения обусловлены различием микропористости, кристалличности образцов и их чувствительностью к газовой атмосфере.